





Recovery of Methanotrophic Activity Is Not Reflected in the Methane-Driven Interaction Network after Peat Mining

Thomas Kaupper,^a Lucas W. Mendes,^b Monica Harnisz,^c Sascha M. B. Krause,^d  Marcus A. Horn,^a  Adrian Ho^a

^aInstitute of Microbiology, Leibniz Universität Hannover, Hannover, Germany

^bCenter for Nuclear Energy in Agriculture, University of São Paulo-USP, São Paulo, Brazil

^cDepartment of Environmental Microbiology, University of Warmia and Mazury in Olsztyn, Olsztyn, Poland

^dZhejiang Tiantong Forest Ecosystem National Observation and Research Station, School of Ecological and Environmental Sciences, East China Normal University, Shanghai, China

ABSTRACT Aerobic methanotrophs are crucial in ombrotrophic peatlands, driving the methane and nitrogen cycles. Peat mining adversely affects methanotrophs, but activity and community composition/abundances may recover after restoration. Considering that the methanotrophic activity and growth are significantly stimulated in the presence of other microorganisms, the methane-driven interaction network, which encompasses methanotrophs and nonmethanotrophs (i.e., the methanotrophic interactome), may also be relevant in conferring community resilience. Yet, little is known of the methanotrophic interactome's response to and recovery from disturbances. Here, we determined the recovery of the methanotrophic interactome as inferred by a co-occurrence network analysis comparing pristine and restored peatlands. We coupled a DNA-based stable isotope probing (SIP) approach using $[^{13}\text{C}]\text{CH}_4$ to a co-occurrence network analysis derived from the ^{13}C -enriched 16S rRNA gene sequences to relate the response in methanotrophic activity to the structuring of the interaction network. Methanotrophic activity and abundances recovered after peat restoration since 2000. "*Methylomonaceae*" taxa were the predominantly active methanotrophs in both peatlands, but the peatlands differed in the relative abundances of *Methyloacidiphilaceae* and *Methylocystis*. However, bacterial community compositions were distinct in both peatlands. Likewise, the methanotrophic interactome was profoundly altered in the restored peatland. Structuring of the interaction network after peat mining resulted in the loss of complexity and modularity, indicating a less connected and efficient network, which may have consequences in the event of recurring/future disturbances. Therefore, determining the response of the methane-driven interaction network, in addition to relating methanotrophic activity to community composition/abundances, provided a more comprehensive understanding of the resilience of the methanotrophs.

IMPORTANCE Microbial resilience against and recovery from disturbances are often determined with regard to microorganisms' activity and community composition/abundances. Rarely has the response of the network of interacting microorganisms been considered, despite accumulating evidence showing that microbial interaction modulates community functioning. Comparing the methane-driven interaction networks of a pristine peatland and a restored peatland, our findings revealed that the metabolically active microorganisms were less connected and formed less-modular "hubs" in the restored peatland, which is indicative of a less complex network that may have consequences with recurring disturbances and environmental changes. This also suggests that the resilience and full recovery in the methanotrophic activity and abundances do not reflect on the interaction network. Therefore, it is relevant to consider the interaction-induced response, in addition to documenting changes in activity and community composition/abundances, to provide a comprehensive understanding of the resilience of microorganisms to disturbances.

Citation Kaupper T, Mendes LW, Harnisz M, Krause SMB, Horn MA, Ho A. 2021. Recovery of methanotrophic activity is not reflected in the methane-driven interaction network after peat mining. *Appl Environ Microbiol* 87:e02355-20. <https://doi.org/10.1128/AEM.02355-20>.

Editor Jeremy D. Semrau, University of Michigan-Ann Arbor

Copyright © 2021 American Society for Microbiology. All Rights Reserved.

Address correspondence to Marcus A. Horn, horn@ifmb.uni-hannover.de, or Adrian Ho, Adrian.ho@ifmb.uni-hannover.de.

Received 23 September 2020

Accepted 7 December 2020

Accepted manuscript posted online 18 December 2020

Published 12 February 2021

KEYWORDS peatland restoration, methane oxidation, methane-based food web, methanotrophs, stable isotope probing

Peat is harvested to meet global fuel and feed demands (e.g., renewable combustible fuel and soil additives [1, 2]). Mining profoundly alters the peat physicochemical properties (e.g., increases pH and compaction and reduces the availability of inorganic compounds [3, 4]), exerting an effect on the indigenous microbial communities with consequences for microbially mediated processes such as greenhouse gas emissions (5, 6). Depending on the mining method (block-cut or vacuum-harvested peat), peat restoration to a pristine-like state can take decades, during which the rewetted peatlands may become a source of carbon, with altered carbon dioxide and methane emissions (3, 7). In particular, methane emission in ombrotrophic peatlands is governed by the balance of methane production in the anoxic peat layers, and aerobic methane oxidation in niches where methane-oxygen counter gradients occur (e.g., the peat-overlying water layer). Hence, aerobic methanotrophs are key to mitigating methane emission in peatlands, acting as a methane biofilter (8). Besides, diazotrophic methanotrophs are a significant source of assimilable nitrogen, driving the N cycle in ombrotrophic peatlands (9–11). Methanotrophs are thus highly relevant members of the peatland microbiome, participating in the C and N cycles. While changes in the abiotic environment following peat restoration have been the focus of earlier work (3, 4), the microbial community composition and abundances, specifically those of methanotrophs, in ombrotrophic peatlands have since gained attention (12–15). Still, less is known about the response of the relevant and metabolically active community members to peat restoration, and it remains to be determined how well the methane-driven network of interacting microorganisms recovers in the reestablished peatland.

Ombrotrophic *Sphagnum*-dominated peatlands are relatively harsh environments that are characterized by low pH and are nutrient depauperate (16). These conditions, along with the antimicrobial properties of *Sphagnum*, may exert pressure to select for specific aerobic methanotrophs (17). Not surprisingly, the methanotrophs, being strongly influenced by their abiotic environment, showed habitat specificity (18, 19). Predominantly active methanotrophs in ombrotrophic peatlands fall into the class *Alphaproteobacteria* (type II methanotrophs), which includes *Methylocystis* and *Methylosinus* (family *Methylocystaceae*), as well as members of the family *Beijerinckiaceae* (*Methylocella*, *Methyloferula*, and *Methylocapsa*); class *Gammaproteobacteria* methanotrophs (type I) belonging to *Methylomonas* and *Methylovulum* were more recently found to be active members of the community (14, 15, 20–23). The methanotrophs form a plethora of interdependent relationships with other organisms, at times supporting multitrophic food webs in high-methane-emission environments (24–27). Accordingly, methane oxidation and growth rates, as well as the transcription of the *pmoA* gene (encoding methane monooxygenase) were significantly stimulated when the methanotrophs were cocultured together with other microorganisms compared to monoculture (28–31). As such, nonmethanotrophs that do not seemingly contribute to methane oxidation are also relevant, indirectly affecting community functioning via interaction-induced effects. Therefore, considering the methane-driven interaction network is important to elaborate community response during peat restoration, but this has so far received little attention.

Here, we aimed to compare and contrast the methane-driven interaction network in ombrotrophic peatlands to follow the recovery in the network structure during peat restoration. Although methanotrophic activity and community composition/abundances may recover after *Sphagnum* regrowth upon peat rewetting (6, 13), the legacy of peat mining may persist in the structure of the interaction network (32, 80). Revisiting the sites of our previous work (pristine and restored peatlands [13]), we performed stable isotope probing (SIP) using [¹³C]CH₄ to track the unidirectional flow of methane into the food web. Instead of deriving the co-occurrence network analysis from isolated DNA (e.g., references 33 and 34), we performed a network analysis using the ¹³C-enriched 16S rRNA gene from SIP to infer the methane-driven interaction network (i.e.,

TABLE 1 Selected physicochemical properties, *pmoA* and 16S rRNA gene abundances, and methane uptake rates in the pristine and restored peatlands^a

Peatland status	pH	Ammonium (mmol · g dry wt ⁻¹)	Nitrate (μmol · g dry wt ⁻¹)	Methane uptake rate (μmol · g dry wt ⁻¹ · day ⁻¹) ^b	<i>pmoA</i> gene abundance (copy no. · g dry wt ⁻¹)	16S rRNA gene abundance (copy no. · g dry wt ⁻¹)	Mean <i>pmoA</i> / 16S rRNA gene abundance (%)
Pristine	4.4 ± 0.19 C	0.2 ± 0.02 C	0.6 ± 0.07 C				
After incubation setup				24.7 ± 6.17 C	(6.0 ± 3.29) × 10 ⁴ C	(6.81 ± 3.41) × 10 ⁷ C	0.08
After replenishing headspace methane				45.6 ± 8.61 A	(3.5 ± 2.47) × 10 ⁵ A	(9.13 ± 4.9) × 10 ⁷ A	0.53
Restored	4.7 ± 0.12 C	0.7 ± 0.08 D	0.7 ± 0.21 C				
After incubation setup				24.7 ± 3.82 C	(4.9 ± 4.02) × 10 ⁵ D	(2.48 ± 0.93) × 10 ⁸ D	0.21
After replenishing headspace methane				31.2 ± 9.57 B	(2.8 ± 1.47) × 10 ⁶ B	(2.52 ± 1.48) × 10 ⁸ B	1.46

^aUppercase letters indicate a level of significance at $P < 0.05$ between sites. C and D refer to data after incubation setup, and A and B refer to data after replenishing headspace methane.

^bMethane uptake rates were determined by linear regression after incubation setup (C and D, $P < 0.05$; days 0 to 8) and after replenishing headspace methane (A and B, $P < 0.05$; days 8 to 13 or 14) (methane depletion curve; see Fig. S1 in the supplemental material).

methanotrophic interactome). We define the methanotrophic interactome as a subset of the entire bacterial community comprising of both methanotrophs and nonmethanotrophs that is tracked via the flow of methane-derived ¹³C. Coupling SIP to the co-occurrence network analysis not only provides direct ecological linkages of the metabolically active members of the interaction network, thereby minimizing spurious and weak connections, but also unambiguously relates community functioning (methane oxidation as the functional response variable) to the network structure.

RESULTS

Comparison of methanotrophic activity and abundance and the abiotic environment in the pristine and restored peatlands. Headspace methane was immediately consumed upon incubation setup (initial and after methane replenishment; see Fig. S1 in the supplemental material) in both peatlands, indicating the presence of a thriving indigenous methanotrophic population. The initial methane uptake rate, reflecting the *in-situ* rate (35), was comparable in both peatlands at ~24 μmol · g dry weight⁻¹ · day⁻¹ (Table 1). This suggests recovery in methanotrophic activity in the restored peatland, consistent with a previous study of the same peatlands over two consecutive years (in 2015 and 2016 [13]). The methane uptake rate increased in both peatlands after replenishing headspace methane, achieving an “induced rate” that was likely caused by population growth during incubation (Table 1) (35). This was corroborated by the increased *pmoA* gene abundance by approximately an order of magnitude after the incubation, indicating methanotrophic growth. Also, the proportion of methanotrophs (i.e., the *pmoA*/16S rRNA gene abundance ratio) increased during the incubation (Table 1). Similarly, the total bacteria, and specifically the methanotrophic population size, recovered to even higher abundances following peat restoration, as was previously documented (13).

The pHs in the two peatlands were comparable, within the range of 4.4 to 4.7 (Table 1). Soluble ammonium was significantly higher after peat restoration, while nitrate concentrations were comparable (Table 1), consistent with previous work (13).

Response of the metabolically active bacterial community composition to peat restoration, as determined by DNA-based SIP. An SIP approach using [¹³C]CH₄ was performed to track the flow of ¹³C into the DNA of metabolically active and replicating microorganisms. Because the methanotrophs are the only microorganisms capable of assimilating methane, ¹³C incorporated into the DNA of nonmethanotrophs indicates the reliance of these microorganisms on methane-derived carbon for growth. Each ultracentrifugation run was performed for DNA extracted from incubations with [¹³C]CH₄ and [unlabelled]CH₄ to distinguish the “heavy” and “light” fractions after amplification of the *pmoA* gene for each gradient fraction (Fig. 1). Admittedly, we cannot completely exclude the presence of unlabeled 16S rRNA gene with a high GC content in

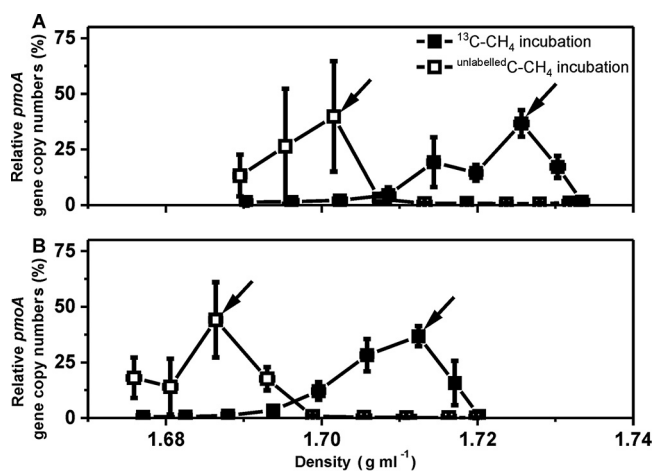


FIG 1 Relative *pmoA* gene abundance along the density gradient of the $[^{13}\text{C}]\text{CH}_4$ and $[\text{unlabelledC}]\text{CH}_4$ incubations from the pristine (A) and restored (B) peatlands (mean \pm standard deviation [SD]; $n=4$). The relative abundance was calculated as the proportion of each fraction over the total sum of the gene abundance for each sample. DNA from the “light” and “heavy” fractions (denoted by arrows) in the $[^{13}\text{C}]\text{CH}_4$ incubations was used for 16S rRNA gene amplicon sequencing.

the heavy fraction (36). The heavy fraction could be clearly separated from the light fraction in both peat incubations (Fig. 1), and this was further supported by the clustering of the distinct communities in both fractions, based on the 16S rRNA gene sequencing analysis (principal-component analysis [PCA]; Fig. 2). Subsequently, co-occurrence network analysis was performed on the ^{13}C -enriched 16S rRNA gene sequences, representing the active community members.

The ^{13}C -enriched bacterial community composition was distinct in the pristine and restored peatlands, indicating that the total community in the restored peatland had not fully recovered to a pristine-like state (Fig. 2). Among the ^{13}C -labeled bacterial phyla, *Proteobacteria* members were predominantly present in both peatlands (>65%; Fig. 3). However, members of the phylum were detected at a significantly higher relative abundance in the restored site (see Fig. S2 in the supplemental material). Within *Proteobacteria*, *Beijerinckiaceae*, *Oligoflexales*, *Polyangiaceae*, *Pajaroellobacter*, *Elsterales*, *Myxococcales*, and *Burkholderiaceae*, as well as the genera *Anaeromyxobacter*, *Occallatibacter*, and *Cavicella* were detected at significantly ($P < 0.05$) differentially higher proportion (overabundant) in the restored compared to that in the pristine peatlands (see Fig. S3 in the supplemental material). However, a member of the *Beijerinckiaceae* (represented by operational taxonomic unit [OTU] 1; Fig. S3) was more abundant in the pristine peatland. Among other phyla, *Acidobacteria*, *Bacteroidetes*, and WPS-2 were present at significantly higher relative abundances in the pristine peatland (Fig. S2). Considering finer taxonomic resolution, differentially higher relative abundances of *Occallatibacter*, *Granulicella*, *Acidimicrobiaceae*, *Acidobacteriales*, “*Candidatus Solibacter*,” and “*Candidatus Koribacter*” belonging to *Acidobacteria*, and *Chitinophagales* within *Bacteroidetes* were detected in the pristine peatland (Fig. S3). WPS-2 is a candidate division represented by an as yet uncultured bacterium. Generally, members of *Acidobacteria* and *Proteobacteria*, along with *Actinobacteria*, are typical active inhabitants of ombrotrophic peatlands (37–39).

The methanotrophs consisted of <2% of the total bacterial population in both peatlands (starting material), based on 16S rRNA gene sequencing analysis (Fig. 3A). After incubation, the methanotrophic population comprised ~20% and ~74% of the total active community (heavy fraction) in the pristine and restored peatland, respectively. The predominantly active methanotrophs, as retrieved from the 16S rRNA gene sequences, belonged to “*Methylomonaceae*” and included the genus *Methylomonas* (>72% of the total methanotrophic population) in both peatlands, whereas the genus

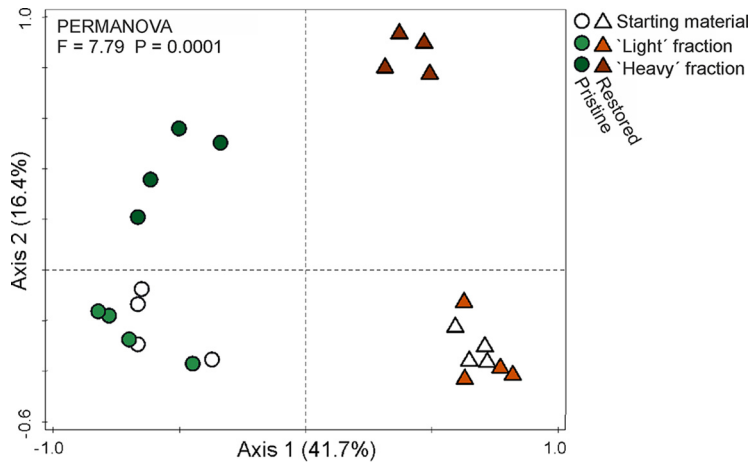


FIG 2 Principal-component analysis showing the clustering of the 16S rRNA gene sequences according to the different fractions (light and heavy) and sites (pristine and restored peatlands) of the incubation with $[^{13}C]CH_4$. The circle and triangle indicate pristine and restored peatlands, respectively.

Methylocystis was relatively more abundant in the restored than the pristine peatland (Fig. 3B). Conversely, *Methylacidiphilaceae* taxa were detected at a higher relative abundance in the pristine than the restored peatland. Although they constituted the majority of the methanotrophic community composition in the starting material, members of *Methylacidiphilaceae* did not assimilate methane as actively as “*Methylomonaceae*” under the incubation conditions; metabolically active *Methylacidiphilaceae* was detected at ~22% and <2% in the heavy fraction of the pristine and restored peatland, respectively, after incubation (Fig. 3).

Insights into the methane-driven co-occurrence interaction network in the pristine and restored peatlands. Subsequently, a co-occurrence network analysis was performed on the ^{13}C -enriched 16S rRNA gene sequences, targeting the community members of the methanotrophic interactome in the pristine and restored peatlands

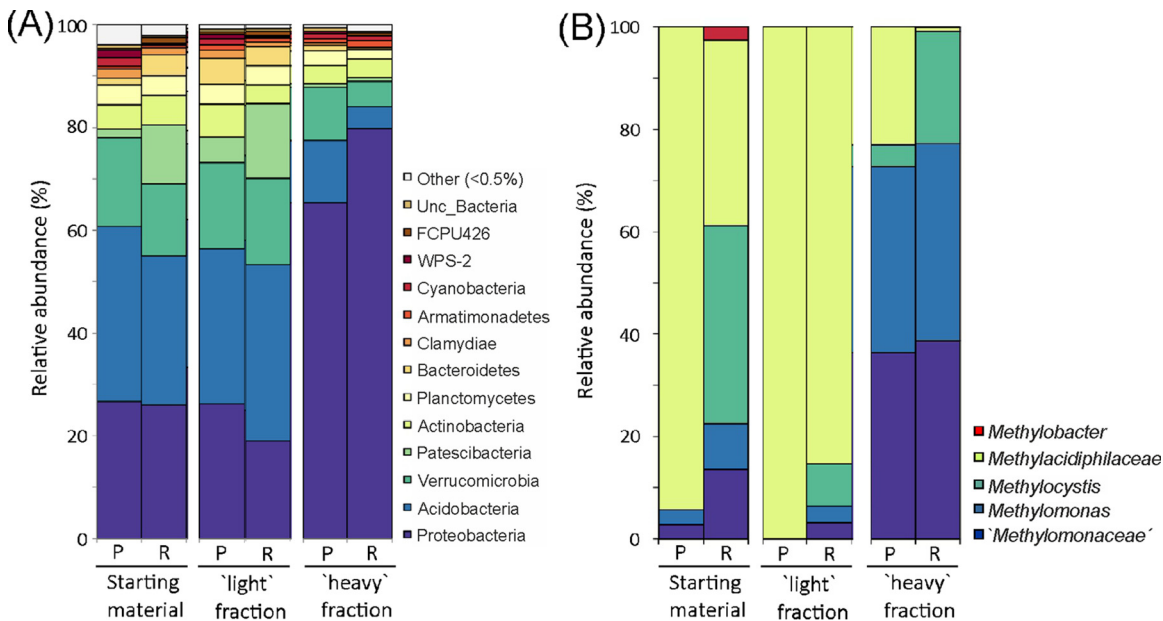


FIG 3 The bacterial (A) and methanotrophic (B) community composition in the starting material (prior to the incubation) and after $[^{13}C]CH_4$ incubation (light and heavy fractions) (mean; $n=4$). The 16S rRNA gene sequences affiliated with methanotrophs in panel B were retrieved from the total community in panel A. The 16S rRNA gene sequences affiliated with the methanotrophs were present at <2% of the total community in the starting material, and at ~20% and ~74%, respectively, in the pristine and restored peatland after incubation (heavy fraction). P and R denote pristine and restored peatlands, respectively.

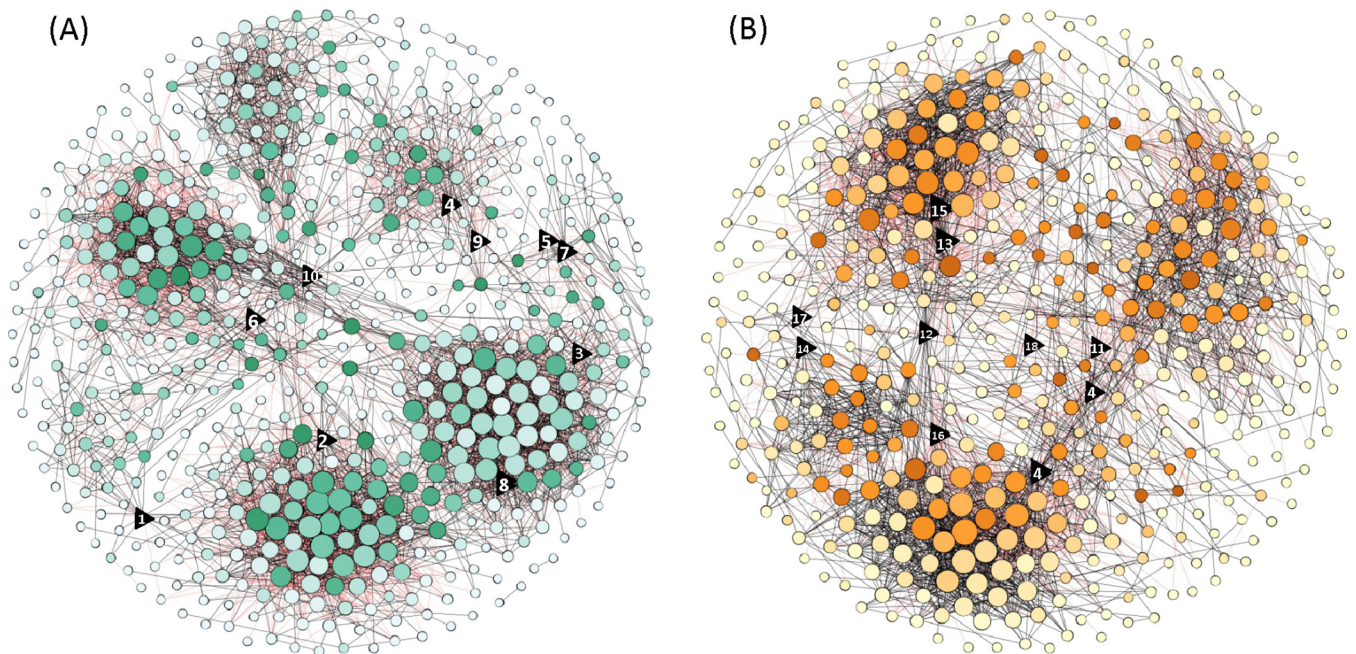


FIG 4 Co-occurrence network analysis in the pristine (A) and restored (B) peatlands. The network analysis was derived from the ^{13}C -enriched 16S rRNA gene sequences (heavy fraction), representing the metabolically active community of the interaction network. The topological properties of the networks are given in Table 2. Significant connection ($P < 0.01$) with a SparCC correlation of a magnitude of more than 0.7 (positive correlation, blue edges) or less than -0.7 (negative correlation, red edges) are given. Each node represents a bacterial taxon at the operational taxonomic unit (OTU) level, given to the lowest taxonomic rank (family, genus, or species) when available. The size of the node is proportional to the number of connections, and a darker shade of a color indicates higher betweenness centrality. The top 10 nodes with the highest betweenness centrality, representing the key nodes, are given as triangles, and the number inside the key nodes refers to their affiliation as follows: 1, *Rhodospirillales*; 2, uncultured bacteria; 3, *Burkholderiaceae*; 4, *Methylomonas* (methanotroph); 5, "*Candidatus Solibacter*"; 6, *Gammaproteobacteria*; 7, *Methylocystis* (methanotroph); 8, *Babeliales*; 9, *Pirellulaceae*; 10, *Methylacidiphilaceae* (methanotroph); 11, *Bdellovibrio*; 12, *Magnetospirillaceae*; 13, *Acidimicrobia*; 14, *Sphingobacteriales*; 15, *Roseiarcus*; 16, *Beijerinckiaceae*; 17, *Myxococcales*; and 18, *Methylomonas paludis* (methanotroph). The OTUs representing the microorganisms and betweenness centrality values of each OTU are listed in Table S1 in the supplemental material.

(Fig. 4). The network topological properties indicate that the pristine peatland harbored a more complex and connected community, exhibiting a higher number of edges (number of connections), degree (number of connections per node or node connectivity), and clustering coefficient (the degree to which the nodes cluster together) than in the restored peatland (Table 2). Accordingly, the pristine peatland also possessed a more diverse metabolically active community (number of significant nodes, representing bacterial taxa at the OTU level), and showed a more modular network structure than the restored peatland (Table 2). Higher modularity is indicative of a more compartmentalized network, having more independently connected groups within the interaction network (40, 41). The network diameter and average path length between co-occurring nodes, indicative of the network efficiency (40, 42), were largely comparable in both peatlands (Table 2). Having a comparatively less complex and connected network structure thus indicates that the methanotrophic interactome in the restored peatland since 2000 had not returned to a pristine-like state, despite the resilience in the methanotrophic activity and abundance.

The nodes with high betweenness centrality were identified as the key nodes (Fig. 4) (43), which likely played a significant regulatory role within the interaction network, affecting methanotrophic activity (44, 45). In particular, the key nodes are not necessarily the more abundant OTUs (Fig. S3), but rather refer to nodes acting as a bridge between other nodes at a relatively higher frequency (43). The 10 key nodes with the highest betweenness centrality were identified in both the pristine and restored peatlands (Fig. 4). Expectedly, these nodes were represented by proteobacterial methanotrophs (*Methylomonas* and *Methylocystis*), as well as by verrucomicrobial methanotrophs belonging to *Methylacidiphilaceae* in the pristine peatland, whereas the methanotroph-related key nodes in the restored peatland were affiliated with *Methylomonas*. It is

TABLE 2 Topological properties of the co-occurrence network analysis in the pristine and restored peatlands

Network properties	Pristine peatland	Restored peatland
No. of nodes ^a	600	464
No. of edges ^b	5,397	3,476
Positive edges (no. [%]) ^c	2,871 (53.2)	2,234 (64.3)
Negative edges (no. [%]) ^d	2,526 (46.8)	1,242 (35.7)
Modularity ^e	7.30	1.82
No. of communities ^f	47	57
Network diam ^g	10	11
Avg path length ^h	4.27	4.30
Avg degree ⁱ	17.99	14.98
Avg clustering coefficient ^j	0.55	0.53

^aMicrobial taxon (at operational taxonomic unit [OTU] level) with at least one significant ($P < 0.01$) and strong (SparCC of more than 0.9 or less than -0.9) correlation.

^bNumber of connections/correlations obtained by SparCC analysis.

^cSparCC positive correlation (more than 0.9 with $P < 0.01$).

^dSparCC negative correlation (less than -0.9 with $P < 0.01$).

^eCapability of the nodes to form highly connected communities, that is, a structure with a high density of between-node connections (inferred by Gephi).

^fA community is defined as a group of nodes densely connected internally.

^gThe longest distance between nodes in the network, measured in number of edges.

^hAverage network distance for all pairs of nodes or the average length of all edges in the network.

ⁱThe average number of connections per node in the network, that is, the node connectivity.

^jHow nodes are embedded in their neighborhood and the degree to which they tend to cluster together.

noteworthy that *Beijerinckiaceae* (phylum *Proteobacteria*), a key node in the restored peatland (Fig. 4), also constitutes methanotrophs harboring soluble methane monooxygenase (sMMO) (*Methylocella*, *Methylocapsa*, and *Methyloferula* [16]), as well as other methylotrophs, but these microorganisms may have been overlooked at the coarse taxonomic resolution. Unexpectedly, many nonmethanotrophs formed the key nodes and appeared to be site specific (Fig. 4). Although they are unable to assimilate methane directly, the nonmethanotrophs also appear to be relevant members of the interaction network.

DISCUSSION

Recovery of the active methanotrophs after peat restoration. Methanotrophic activity and population size recovered after peat restoration when pristine and restored sites were compared (Table 1). Likewise, pH and nitrate concentrations returned to pristine-like levels, but ammonium concentrations remained significantly higher in the restored site. These trends were also documented in a previous study of the same sites sampled in 2015 and 2016, suggesting the presence of a relatively persistent methanotrophic population, possibly attributable to narrow fluctuations in environmental conditions (13). It thus appears that the methanotrophs recovered <15 years after *Sphagnum* reestablished during peat restoration.

The metabolically active bacterial community composition, including the methanotrophs, was determined by targeting the ^{13}C -enriched 16S rRNA gene after $[^{13}\text{C}]\text{CH}_4$ SIP. Predominantly active methanotrophs belonged to "*Methylomonaceae*" ($>72\%$ of the methanotrophic community composition) in both peatlands, while *Methylacidiphilaceae* and *Methylocystis* formed the rest of the methanotrophic community (Fig. 3). In particular, *Methylocystis* is thought to possess ecological traits suitable for the relatively inhospitable and fluctuating environmental conditions in ombrotrophic peatlands, having the metabolic potential to fix N_2 , utilize other substrates besides methane (e.g., acetate), and being favored by the lower pH (23, 46–48). Besides *Methylocystis*, members of "*Methylomonaceae*" (e.g., *Methylomonas* strains) and *Methylacidiphilaceae* (e.g., *Methyloacidiphilum fumarolicum* SolV), which also formed the active community, are also potentially diazotrophic, as indicated by the presence of the *nifH* gene (encoding nitrogenase) (49, 50). Consistent with previous studies, active gammaproteobacterial methanotrophs (namely, *Methylomonas* and

Methylovulum) have also been found to codominate alongside *Methylocystis* in some peatlands (14, 20, 21). This suggests that traits to grow and survive in acidic peatlands are not confined to a particular methanotroph subgroup.

Previously, we characterized the methanotrophic community composition in the pristine and restored sites (same sites as in this study), along with the community in an actively mined peatland and those in abandoned peatlands since 2004 and 2009 (13). The methanotrophic community composition in the restored peatland resembled those in the pristine peatland, clustering more closely together as shown in a correspondence analysis (13). This indicates that the methanotrophic community composition recovered following peat restoration. Here, although the relative abundances of *Methylacidiphilaceae* and *Methylocystis* species differed in the pristine and restored peatlands, the predominantly active methanotrophs comprised the same family members (Fig. 3). However, the active bacterial community composition in response to methane was distinct in both peatlands (Fig. 2 and 3). Hence, specific microbial subpopulations may have shown relatively faster recovery than the total bacterial community composition after peat mining.

Insights into the recovery of the methanotrophic interactome after peat restoration. The recovery in the methanotrophic activity and community composition/abundances was not reflected in the structure of the interaction network, even after approximately 2 decades of peat rewetting (Table 2 and Fig. 4). The pristine peatland harbored a more complex methanotrophic interactome, possessing a higher number of nodes with significant correlations, edges, degree, and clustering coefficient, as well as having higher modularity (Table 2). These topological features are indicative of a more connected and robust network (42, 51, 52) and suggest that the methanotrophic interactome in the pristine peatland was characterized by relatively higher metabolic exchange and competition among community members that likely increased their co-occurrence (53, 54). Also, having relatively higher modularity in the pristine peatland is anticipated to constrain the effects of environmental stressors/disturbance on localized areas (compartments) within the network (55). In contrast, the loss of modularity in the restored peatland suggests that stress effects would be more uniformly distributed among community members, which may become more vulnerable in the face of intensified or recurring disturbances (51, 56). Hence, the methane-driven community in the restored peatland may not be as resilient as the community in the pristine peatland in responding to future changes in environmental conditions. Indeed, a recent study showed the unraveling of the methanotrophic interactome concomitant to significantly impair methanotrophic activity following NH_4Cl -induced stressor intensification (56). Overall, considering the co-occurrence network analysis in addition to activity measurements and characterization of the community composition/abundances may provide a more comprehensive understanding, moving beyond the diversity-ecosystem functioning relationship (e.g., reference 57), to encompass potential interaction-induced effects.

Admittedly, we could not account for seasonal variations affecting the interaction networks. However, the consistent trends in methanotrophic activity and community composition/abundances in the pristine and restored peatlands in previous (sampled in August 2015 and June 2016 [13]) and current work (May 2019; Table 1), despite a 3-year interval, suggest that a specific methanotrophic population persists over time. Although we anticipate a relatively consistent methanotrophic population, the seasonal dynamics of the interaction network warrant attention in future studies.

The methanotrophs are the only microbial group capable of assimilating methane, having the role of a "primary" producer, whereby the methane-derived carbon is anticipated to fuel the community. Nevertheless, the methanotrophs may gain from other members of the interactome (e.g., stimulation of methanotrophic growth by cobalamin excreted by other microorganisms [58]), which may have been inadvertently excluded by the experimental design capturing the unidirectional flow of ^{13}C . Expectedly, the key nodes included the methanotrophs (Fig. 4). Surprisingly, the key nodes were overwhelmingly represented by the nonmethanotrophs and were distinct in the pristine

and restored peatlands. This indicates sufficiently redundant community members sharing traits to fulfill similar roles ensuring community functioning within the methanotrophic interactome (33, 41). It is not unreasonable to assume that selective predation on the methanotrophs may have occurred (59). For instance, members of *Myxococcales*, a key taxon in the restored peat, have been widely recognized as predators, swarming their prey in a coordinated and cooperative manner during feeding (60). *Beijerinckiaceae*, another key taxon, includes nonmethanotrophic methylotrophs which likely benefited from (intermediary) products of methane oxidation (e.g., methanol, formaldehyde, and formate). Hence, the cross-feeding between methanotrophs and nonmethanotrophic methylotrophs (e.g., *Methylotenera*) drives their co-occurrence (26, 56). It is noteworthy that *Beijerinckiaceae* also includes methanotrophs, but the methanotrophs and nonmethanotrophic methylotrophs could not be distinguished at the taxonomic resolution in this study. Also, *Burkholderiaceae* may comprise microorganisms shown to have a stimulatory effect on methanotrophic growth in cocultures (i.e., *Cupriavidus* [29]). Although some of the key taxa (e.g., *Burkholderiaceae*, *Sphingobacteriales*, *Beijerinckiaceae*, and *Bdellovibrio*) have been identified to co-occur alongside and interact with the methanotrophs (29, 56, 61), the underlying mechanisms driving the biological interaction and organization (e.g., commensalism and mutualism [62, 63]) warrant further probing by isolation and coculture studies (64). Despite lacking the metabolic capability to assimilate methane, the detection of the nonmethanotrophs as key nodes indicate their potentially significant role within the interaction network. In particular, the key nodes in the restored peatlands may act to expedite the natural restoration process (65).

Conclusion. We elaborated on the methane-driven interaction network after peat mining by comparing a pristine and restored peatland. Our findings showed the structuring of the interaction network resulting in the loss of complexity, connectedness, and modularity in the restored peatland, which may have consequences in the face of future disturbances and environmental changes. They also suggest that the reestablished peatlands had not yet fully recovered, despite showing resilience in methanotrophic activity. More generally, our study suggests the inclusion of interaction-induced responses, in addition to documenting shifts in community composition/abundances, as a step forward to understand the resilience of microbial communities to disturbances.

MATERIALS AND METHODS

Peat sampling and incubation setup. The sampling sites are ombrotrophic peatlands located in Warmia and Mazury Province, Poland. The upper ~10 cm of peat below the water surface was collected in May 2019 from a pristine peatland (Zielony Mechacz; 53°54'24"N, 19°41'41"E) and was regarded as the reference site for comparison to the restored peatland (Rucianka; 54°15'34"N, 19°44'0.4"E). These peatlands were selected based on a previous study showing recovery in the methanotrophic activity and abundances after peat mining (13). The atmospheric temperature at the time of sampling was 21 to 25°C. Five cores (10-cm height × 3.5-cm diameter) were sampled from four randomly selected plots (spaced >4 m apart) from each site and composited, giving four independent replicates per site. The pristine peatland was declared a nature reserve since 1962, while peatland in the restored site was dammed, rewetted, and remained waterlogged since 2000 after peat excavation using the block peat method. In both sites, *Sphagnum* spp. (e.g., *Sphagnum fimbriatum*, *Sphagnum fluuosum*, *Sphagnum fallax*, and *Sphagnum capillifolium*) dominated the vegetation, interspersed with *Orthotrichum lyellii*. The pH in both peatlands was within a narrow range of 4.4 to 4.7. Detailed peat hydrology and selected physicochemical parameters are given elsewhere (Table 1) (13). The samples were transported to the laboratory with coolers in ice.

Each incubation containing 5 g fresh sample in a 120-ml bottle was performed in eight replicates for the pristine and restored peat. After sealing the bottle with a butyl rubber stopper and crimp cap, the headspace methane concentration in the bottle was adjusted to ~2% (vol/vol) [^{unlabelled}C]CH₄ or [¹³C]CH₄ (*n* = 4 each) in air. Incubation was performed at 27°C while shaking (110 rpm) in the dark. Headspace methane concentration was monitored during the incubation. Upon methane depletion, headspace was replenished with 2% (vol/vol) [^{unlabelled}C]CH₄ or [¹³C]CH₄ in air, and incubation was resumed under the same conditions as before. Incubation was terminated after approximately 30 μmol CH₄ · g fresh sample⁻¹ was consumed (13 to 14 days; see Fig. S1 in the supplemental material) to ensure sufficient ¹³C labeling (66). The samples were immediately homogenized and collected after incubation to be stored in the -20°C freezer until DNA extraction.

Methane and inorganic N measurements. Headspace methane was monitored daily using a gas chromatograph (7890B GC system; Agilent Technologies, Santa Clara, CA) coupled to a pulsed discharge

helium ionization detector (PD-HID). Helium was used as the carrier gas. The methane uptake rate was determined by linear regression. The gravimetric water content (~93% in both peat samples) was determined after drying the peat in the 70°C oven until the weight remained constant. Soluble ammonium and nitrate were determined colorimetrically in autoclaved deionized water (1:1 wt/vol) as described before (67, 68) using an Infinite M Plex reader (Tecan, Männedorf, Switzerland).

DNA extraction and quantitative PCR. DNA was extracted using the DNeasy PowerSoil kit (Qiagen, Hilden, Germany) according to the manufacturer's instructions. A *pmoA* gene-targeted quantitative PCR (qPCR) assay (A189f/mb661r primer pair) was performed to enumerate methanotroph abundance. Additionally, a qPCR targeting the 16S rRNA gene (341F/907R primer pair) was performed to determine the abundance of the total bacterial population. Both qPCR assays were performed using the CFX Connect real-time PCR system (Bio-Rad, Hercules, CA). The *pmoA* gene-targeted qPCR was performed as described before (69) with minor modifications (70); the reagents and reagent concentrations, as well as the PCR thermal profile for the qPCR assay, are given elsewhere (70). Each reaction in the 16S rRNA gene-targeted qPCR (total volume, 20 μ l) consisted of 10 μ l SensiMix (2 \times), 1.2 μ l MgCl₂ (50 mM), 1 μ l bovine serum albumin (BSA; 1%), 2 μ l of each primer (10 μ M), 1.8 μ l of H₂O, and 2 μ l of template DNA. The PCR thermal profile consisted of an initial denaturation step at 95°C for 8 min, followed by 45 cycles of denaturation at 95°C for 15 s, annealing at 55.7°C for 15 s, and elongation at 72°C for 40 s, with an additional data acquisition step at 80°C for 8 s. The template DNA from the peat (starting material and after incubation) was diluted 50-fold (mean total DNA, 13.5 to 46.5 ng DNA \cdot μ l⁻¹) for both qPCR assays to determine the *pmoA*/16S rRNA gene abundance ratio (Table 1), while template DNA to determine the relative *pmoA* gene abundance after fractionation for the SIP analysis was undiluted (see "[¹³C]CH₄ stable isotope probing," below). The calibration curve (10¹ to 10⁸ *pmoA* or 16S rRNA gene copy numbers) was derived from the gene library (71, 72). The specificity of the amplicons was determined from the melt curve and further verified on 1% agarose gel electrophoresis, showing a single band of the correct size. The qPCR efficiency was 94.3%, with an *R*² of 0.988.

[¹³C]CH₄ stable isotope probing. Isopycnic ultracentrifugation (144,000 \times *g* for 67 h) was performed using the Optima L-80XP ultracentrifuge (Beckman Coulter, Inc., USA) as described before (66). Briefly, fractionation was immediately performed after ultracentrifugation using a peristaltic pump (3 rpm \cdot min⁻¹), yielding 10 or 11 fractions, from which the final fraction was discarded. The density of each fraction was determined using an AR200 digital refractometer (Reichert Technologies, Munich, Germany). DNA was precipitated by introducing two washing steps with ethanol, and the pellet was suspended in 30 μ l ultrapure PCR water (Invitrogen, Waltham, MA). Thereafter, the *pmoA* gene was enumerated from each fraction using the qPCR assay described above to distinguish the light from the heavy fraction by comparing the DNA retrieved from the [¹³C]CH₄ and [unlabelledC]CH₄ incubations (Fig. 1). The 16S rRNA genes from the light and heavy fractions, as well that as from the starting material, were subsequently amplified for Illumina MiSeq sequencing.

16S rRNA gene amplicon sequencing. The 16S rRNA gene was amplified using the primer pair 341F/805R, as detailed before (56). Briefly, each PCR comprised 20 μ l 2 \times Kapa HiFi HotStart ready mix (Roche, Mannheim, Germany), 2 μ l each forward/reverse tagged-primers (10 μ M), 2 μ l BSA (1%), and 4 μ l DNA template. PCR-grade water was added to achieve a total volume of 40 μ l. The PCR thermal profile consisted of an initial denaturation step at 94°C for 7 min, followed by 30 cycles of denaturation at 94°C for 30 s, annealing at 53°C for 30 s, and elongation at 72°C for 30 s. The final elongation step was at 72°C for 5 min. The amplicons were purified using the GeneRead size selection kit (Qiagen, Hilden, Germany) after verification on 1% agarose gel electrophoresis. Thereafter, a second PCR was performed using 5 μ l of template from the first PCR to attach the adapters to the 16S rRNA gene amplicon using the Nextera XT index kit (Illumina, San Diego, CA). The PCR reagents, reagent concentrations, and thermal profile for the second PCR are given elsewhere (56). Following the second PCR, the 16S rRNA gene amplicon was purified using the MagSi-NGS^{PREP} Plus magnetic beads (Steinbrenner Laborsysteme GmbH, Wiesenbach, Germany) according to the manufacturer's instructions. After purification, equimolar amounts of 16S rRNA gene amplicons (133 ng) were pooled for library preparation and sequencing (Illumina MiSeq version 3 chemistry, paired-end, and 600 cycles).

16S rRNA gene sequencing analysis. The 16S rRNA gene sequences were processed using QIIME 2 version 2019.10, as described before (56). Briefly, after merging the paired-end reads using PEAR (73), the sequences were demultiplexed, and quality control was performed with DADA2 (74) to remove remaining chimeric and low-quality sequences. Approximately 1,010,000 high-quality contigs (on average, 31,604 contigs per sample) were obtained. After removing singletons and doubletons, the samples were rarefied to 18,800 contigs, following the number of the sample with the lowest contigs. The classification was performed at 97% similarity against the Silva database version 132 (75); the generated matrix based on the relative abundance of the OTUs was further used for statistical analyses. The affiliations of the OTUs are given to the lowest taxonomic rank (family, genus, or species), whenever possible.

A principal-component analysis (PCA) was performed to assess the separation of the ¹³C-enriched (active) from the unlabelledC (inactive) bacterial community composition and to determine the recovery of the community composition following peat restoration. The PCA was constructed using Canoco version 4.5 (Biometrics, Wageningen, the Netherlands). To test the significance of the PCA clustering, permutational multivariate analysis of variance (PERMANOVA) was performed with the software PAST version 4.01 (76). Furthermore, the differential relative abundances of (overabundant) OTUs in the restored versus the pristine peatlands were determined using STAMP software (77). The *P* values were calculated based on the two-sided Welch's *t* test and corrected using the Benjamini-Hochberg false-discovery rate.

Additionally, a co-occurrence network analysis was performed using the ¹³C-enriched 16S rRNA gene sequences to explore potential interaction among the active members of the methanotrophic

interactome. The network analysis was performed using the Python module SparCC, and the network properties were calculated with Gephi (Table 2) (78). The same analytical pipeline was applied to each network (pristine and restored peatlands). The *P* values were obtained by 99 permutations of random selections of the data table for each network. The true SparCC nonrandom correlations were selected based on a magnitude of more than 0.7 or less than -0.7 , with a statistical significance of $P < 0.01$. Comparison between the networks was assessed based on their topological properties namely, the number of nodes, edges, modularity, number of communities, average path length, network diameter, average degree, and clustering coefficient (Table 2) (79). Furthermore, the OTUs with high betweenness centrality, i.e., the number of times a node acts as a bridge along the shortest path between two other nodes, were determined (43). These nodes are regarded as key nodes, representing microorganisms that likely play a significant role within the methanotrophic interactome (44).

Statistical analyses. Normal distribution was tested using the Kolmogorov-Smirnov test at $P = 0.05$. Equal distribution of variance was tested and one-sided *t* tests ($P = 0.05$) were then performed comparing the pristine and restored peatlands. Where anormal distribution was not met, a Mann-Whitney U test was performed.

Data availability. 16S rRNA gene sequences were deposited at the National Center for Biotechnology Information (NCBI) under the accession numbers [SRR12542333](https://doi.org/10.1093/bioinformatics/btad001) to [SRR12542364](https://doi.org/10.1093/bioinformatics/btad001) (project number [PRJNA659768](https://doi.org/10.1093/bioinformatics/btad001)).

SUPPLEMENTAL MATERIAL

Supplemental material is available online only.

SUPPLEMENTAL FILE 1, PDF file, 4.9 MB.

ACKNOWLEDGMENTS

T.K. and A.H. are financially supported by the Deutsche Forschungsgemeinschaft (grant HO6234/1-1). A.H. and M.A.H. are also financially supported by the Leibniz Universität Hannover, Germany.

We declare no conflict of interest.

REFERENCES

1. Cleary J, Roulet NT, Moore TR. 2005. Greenhouse gas emissions from Canadian peat extraction, 1990–2000: a life-cycle analysis. *AMBIO* 34:456–461. <https://doi.org/10.1579/0044-7447-34.6.456>.
2. Pryce S. 1991. Alternatives to peat. *Prof Hort* 5:101–106.
3. Basiliko N, Blodau C, Roehm C, Bengtson P, Moore TR. 2007. Regulation of decomposition and methane dynamics across natural, commercially mined, and restored northern peatlands. *Ecosystems* 10:1148–1165. <https://doi.org/10.1007/s10021-007-9083-2>.
4. Andersen R, Francez A-J, Rochefort L. 2006. The physicochemical and microbiological status of a restored bog in Québec: identification of relevant criteria to monitor success. *Soil Biol Biochem* 38:1375–1387. <https://doi.org/10.1016/j.soilbio.2005.10.012>.
5. Juottonen H, Hynninen A, Nieminen M, Tuomivirta TT, Tuittila E-S, Nousiainen H, Kell DK, Yrjälä K, Tervahauta A, Fritze H. 2012. Methane-cycling microbial communities and methane emission in natural and restored peatlands. *Appl Environ Microbiol* 78:6386–6389. <https://doi.org/10.1128/AEM.00261-12>.
6. Putkinen A, Tuittila E-S, Siljanen HMP, Bodrossy L, Fritze H. 2018. Recovery of methane turnover and the associated microbial communities in restored cutover peatlands is strongly linked with increasing *Sphagnum* abundance. *Soil Biol Biochem* 116:110–119. <https://doi.org/10.1016/j.soilbio.2017.10.005>.
7. Holl D, Pfeiffer E-M, Kutzbach L. 2020. Comparison of eddy covariance CO₂ and CH₄ fluxes from mined and recently rewetted sections in a north-western German cutover bog. *Biogeosciences* 17:2853–2874. <https://doi.org/10.5194/bg-17-2853-2020>.
8. Yavitt JB, Lang GE, Downey DM. 1988. Potential methane production and methane oxidation rates in peatland ecosystems of the Appalachian Mountains, United States. *Global Biogeochem Cycles* 2:253–268. <https://doi.org/10.1029/GB002i003p00253>.
9. Ho A, Le Bodelier P. 2015. Diazotrophic methanotrophs in peatlands: the missing link? *Plant Soil* 389:419–423. <https://doi.org/10.1007/s11104-015-2393-9>.
10. Larmola T, Leppänen SM, Tuittila E-S, Aarva M, Merilä P, Fritze H, Tirola M. 2014. Methanotrophy induces nitrogen fixation during peatland development. *Proc Natl Acad Sci U S A* 111:734–739. <https://doi.org/10.1073/pnas.1314284111>.
11. Vile MA, Kelman Wieder R, Živković T, Scott KD, Vitt DH, Hartssock JA, Iosue CL, Quinn JC, Petix M, Fillingim HM, Popma JMA, Dynarski KA, Jackman TR, Albright CM, Wyckoff DD. 2014. N₂-fixation by methanotrophs sustains carbon and nitrogen accumulation in pristine peatlands. *Biogeochemistry* 121:317–328. <https://doi.org/10.1007/s10533-014-0019-6>.
12. Kip N, van Winden JF, Pan Y, Bodrossy L, Reichart G-J, Smolders AJP, Jetten MSM, Damsté JSS, Op den Camp HJM. 2010. Global prevalence of methane oxidation by symbiotic bacteria in peat-moss ecosystems. *Nature Geosci* 3:617–621. <https://doi.org/10.1038/ngeo939>.
13. Reumer M, Harnisz M, Lee HJ, Reim A, Grunert O, Putkinen A, Fritze H, Bodelier PLE, Ho A. 2017. Impact of peat mining and restoration on methane turnover potential and methane-cycling microorganisms in a northern bog. *Appl Environ Microbiol* 84:e02218-17. <https://doi.org/10.1128/AEM.02218-17>.
14. Esson KC, Lin X, Kumaresan D, Chanton JP, Murrell JC, Kostka JE. 2016. Alpha- and gammaproteobacterial methanotrophs codominate the active methane-oxidizing communities in an acidic boreal peat bog. *Appl Environ Microbiol* 82:2363–2371. <https://doi.org/10.1128/AEM.03640-15>.
15. Liebner S, Svenning MM. 2013. Environmental transcription of *mmoX* by methane-oxidizing proteobacteria in a subarctic peatland. *Appl Environ Microbiol* 79:701–706. <https://doi.org/10.1128/AEM.02292-12>.
16. Dedysh SN. 2011. Cultivating uncultured bacteria from northern wetlands: knowledge gained and remaining gaps. *Front Microbiol* 2:184. <https://doi.org/10.3389/fmicb.2011.00184>.
17. Kostka JE, Weston DJ, Glass JB, Lilleskov EA, Shaw AJ, Turetsky MR. 2016. The *Sphagnum* microbiome: new insights from an ancient plant lineage. *New Phytol* 211:57–64. <https://doi.org/10.1111/nph.13993>.
18. Kaupper T, Luehrs J, Lee HJ, Mo Y, Jia Z, Horn MA, Ho A. 2020. Disentangling abiotic and biotic controls of aerobic methane oxidation during recolonization. *Soil Biol Biochem* 142:107729. <https://doi.org/10.1016/j.soilbio.2020.107729>.
19. Knief C. 2015. Diversity and habitat preferences of cultivated and uncultivated aerobic methanotrophic bacteria evaluated based on *pmoA* as molecular marker. *Front Microbiol* 6:1346. <https://doi.org/10.3389/fmicb.2015.01346>.
20. Chen Y, Dumont MG, Neufeld JD, Bodrossy L, Stralis-Pavese N, McNamara NP, Ostle N, Briones MJL, Murrell JC. 2008. Revealing the uncultivated majority: combining DNA stable-isotope probing, multiple displacement amplification and metagenomic analyses of uncultivated *Methylocystis* in acidic

- peatlands. *Environ Microbiol* 10:2609–2622. <https://doi.org/10.1111/j.1462-2920.2008.01683.x>.
21. Gupta V, Smemo KA, Yavitt JB, Basiliko N. 2012. Active methanotrophs in two contrasting North American peatland ecosystems revealed using DNA-SIP. *Microb Ecol* 63:438–445. <https://doi.org/10.1007/s00248-011-9902-z>.
 22. Danilova OV, Kulichevskaya IS, Rozova ON, Detkova EN, Bodelier PLE, Trotsenko YA, Dedysh SN. 2013. *Methylomonas paludis* sp. nov., the first acid-tolerant member of the genus *Methylomonas*, from an acidic wetland. *Int J Syst Evol Microbiol* 63:2282–2289. <https://doi.org/10.1099/ijls.0.045658-0>.
 23. Belova SE, Baani M, Suzina NE, Bodelier PLE, Liesack W, Dedysh SN. 2011. Acetate utilization as a survival strategy of peat-inhabiting *Methylocystis* spp. *Environ Microbiol Rep* 3:36–46. <https://doi.org/10.1111/j.1758-2229.2010.00180.x>.
 24. Ho A, Angel R, Veraart AJ, Dumont MG, McDonald IR, Murrell JC. 2004. Analysis of methanotrophic bacteria in Movile Cave by stable isotope probing. *Environ Microbiol* 6:111–120. <https://doi.org/10.1046/j.1462-2920.2003.00543.x>.
 25. Ho A, Angel R, Veraart AJ, Daebeler A, Jia Z, Kim SY, Kerckhof F-M, Boon N, Bodelier PLE. 2016. Biotic interactions in microbial communities as modulators of biogeochemical processes: methanotrophy as a model system. *Front Microbiol* 7:1285. <https://doi.org/10.3389/fmicb.2016.01285>.
 26. Krause SMB, Johnson T, Samadhi Karunaratne Y, Fu Y, Beck DAC, Chistoserdova L, Lidstrom ME. 2017. Lanthanide-dependent cross-feeding of methane-derived carbon is linked by microbial community interactions. *Proc Natl Acad Sci U S A* 114:358–363. <https://doi.org/10.1073/pnas.1619871114>.
 27. Agasild H, Zingel P, Tuvikene L, Tuvikene A, Timm H, Feldmann T, Salujõe J, Toming K, Jones RI, Nöges T. 2014. Biogenic methane contributes to the food web of a large, shallow lake. *Freshw Biol* 59:272–285. <https://doi.org/10.1111/fwb.12263>.
 28. Ho A, Roy K, de Thas O, de Neve J, Hoefman S, Vandamme P, Heylen K, Boon N. 2014. The more, the merrier: heterotroph richness stimulates methanotrophic activity. *ISME J* 8:1945–1948. <https://doi.org/10.1038/ismej.2014.74>.
 29. Stock M, Hoefman S, Kerckhof F-M, Boon N, de Vos P, de Baets B, Heylen K, Waegeman W. 2013. Exploration and prediction of interactions between methanotrophs and heterotrophs. *Res Microbiol* 164:1045–1054. <https://doi.org/10.1016/j.resmic.2013.08.006>.
 30. Jeong S-Y, Cho K-S, Kim TG. 2014. Density-dependent enhancement of methane oxidation activity and growth of *Methylocystis* sp. by a non-methanotrophic bacterium *Shingopyxis* sp. *Biotechnol Rep (Amst)* 4:128–133. <https://doi.org/10.1016/j.btre.2014.09.007>.
 31. Veraart AJ, Garbeva P, van Beersum F, Ho A, Hordijk CA, Meima-Franke M, Zweepers AJ, Bodelier PLE. 2018. Living apart together-bacterial volatiles influence methanotrophic growth and activity. *ISME J* 12:1163–1166. <https://doi.org/10.1038/s41396-018-0055-7>.
 32. Pérez-Valera E, Goberna M, Faust K, Raes J, García C, Verdú M. 2017. Fire modifies the phylogenetic structure of soil bacterial co-occurrence networks. *Environ Microbiol* 19:317–327. <https://doi.org/10.1111/1462-2920.13609>.
 33. Barberán A, Bates ST, Casamayor EO, Fierer N. 2012. Using network analysis to explore co-occurrence patterns in soil microbial communities. *ISME J* 6:343–351. <https://doi.org/10.1038/ismej.2011.119>.
 34. Mo Y, Jin F, Zheng Y, Baoyin T, Ho A, Jia Z. 2020. Succession of bacterial community and methanotrophy during lake shrinkage. *J Soils Sediments* 20:1545–1557. <https://doi.org/10.1007/s11368-019-02465-6>.
 35. Steenbergh AK, Meima MM, Kamst M, Bodelier PLE. 2010. Biphasic kinetics of a methanotrophic community is a combination of growth and increased activity per cell. *FEMS Microbiol Ecol* 71:12–22. <https://doi.org/10.1111/j.1574-6941.2009.00782.x>.
 36. Lueders T, Manefield M, Friedrich MW. 2004. Enhanced sensitivity of DNA- and rRNA-based stable isotope probing by fractionation and quantitative analysis of isopycnic centrifugation gradients. *Environ Microbiol* 6:73–78. <https://doi.org/10.1046/j.1462-2920.2003.00536.x>.
 37. Palmer K, Horn MA. 2012. Actinobacterial nitrate reducers and proteobacterial denitrifiers are abundant in N₂O-metabolizing peat. *Appl Environ Microbiol* 78:5584–5596. <https://doi.org/10.1128/AEM.00810-12>.
 38. Deng Y, Cui X, Hernández M, Dumont MG. 2014. Microbial diversity in hummock and hollow soils of three wetlands on the Qinghai-Tibetan Plateau revealed by 16S rRNA pyrosequencing. *PLoS One* 9:e103115. <https://doi.org/10.1371/journal.pone.0103115>.
 39. Ivanova AA, Wegner C-E, Kim Y, Liesack W, Dedysh SN. 2016. Identification of microbial populations driving biopolymer degradation in acidic peatlands by metatranscriptomic analysis. *Mol Ecol* 25:4818–4835. <https://doi.org/10.1111/mec.13806>.
 40. Zhou J, Deng Y, Luo F, He Z, Tu Q, Zhi X. 2010. Functional molecular ecological networks. *mBio* 1:e00169-10. <https://doi.org/10.1128/mBio.00169-10>.
 41. Williams RJ, Howe A, Hofmøckel KS. 2014. Demonstrating microbial co-occurrence pattern analyses within and between ecosystems. *Front Microbiol* 5:358. <https://doi.org/10.3389/fmicb.2014.00358>.
 42. Bissett A, Brown MV, Siciliano SD, Thrall PH. 2013. Microbial community responses to anthropogenically induced environmental change: towards a systems approach. *Ecol Lett* 16(Suppl 1):128–139. <https://doi.org/10.1111/ele.12109>.
 43. Poudel R, Jumpponen A, Schlatter DC, Paulitz TC, Gardener BBM, Kinkel LL, Garrett KA. 2016. Microbiome networks: a systems framework for identifying candidate microbial assemblages for disease management. *Phytopathology* 106:1083–1096. <https://doi.org/10.1094/PHYTO-02-16-0058-FI>.
 44. Borgatti SP. 2005. Centrality and network flow. *Social Networks* 27:55–71. <https://doi.org/10.1016/j.socnet.2004.11.008>.
 45. van der Heijden MGA, Hartmann M. 2016. Networking in the plant microbiome. *PLoS Biol* 14:e1002378. <https://doi.org/10.1371/journal.pbio.1002378>.
 46. Im J, Lee S-W, Yoon S, DiSpirito AA, Semrau JD. 2011. Characterization of a novel facultative *Methylocystis* species capable of growth on methane, acetate and ethanol. *Environ Microbiol Rep* 3:174–181. <https://doi.org/10.1111/j.1758-2229.2010.00204.x>.
 47. Han D, Dedysh SN, Liesack W. 2018. Unusual genomic traits suggest *Methylocystis bryophila* S285 to be well adapted for life in peatlands. *Genome Biol Evol* 10:623–628. <https://doi.org/10.1093/gbe/evy025>.
 48. Zhao J, Cai Y, Jia Z. 2020. The pH-based ecological coherence of active canonical methanotrophs in paddy soils. *Biogeosciences* 17:1451–1462. <https://doi.org/10.5194/bg-17-1451-2020>.
 49. Khadem AF, Pol A, Wiczeorek A, Mohammadi SS, Francois J-K, Stunnenberg HG, Jetten MSM, Op den Camp HJM. 2011. Autotrophic methanotrophy in verrucomicrobia: *Methylacidiphilum fumarolicum* SolV uses the Calvin-Benson-Bassham cycle for carbon dioxide fixation. *J Bacteriol* 193:4438–4446. <https://doi.org/10.1128/JB.00407-11>.
 50. Auman AJ, Speake CC, Lidstrom ME. 2001. *nifH* sequences and nitrogen fixation in type I and type II methanotrophs. *Appl Environ Microbiol* 67:4009–4016. <https://doi.org/10.1128/aem.67.9.4009-4016.2001>.
 51. Faust K, Raes J. 2012. Microbial interactions: from networks to models. *Nat Rev Microbiol* 10:538–550. <https://doi.org/10.1038/nrmicro2832>.
 52. Mendes LW, Raaijmakers JM, de Hollander M, Mendes R, Tsai SM. 2018. Influence of resistance breeding in common bean on rhizosphere microbiome composition and function. *ISME J* 12:212–224. <https://doi.org/10.1038/ismej.2017.158>.
 53. van Elsas JD, Chiurazzi M, Mallon CA, Elhottova D, Kristufek V, Salles JF. 2012. Microbial diversity determines the invasion of soil by a bacterial pathogen. *Proc Natl Acad Sci U S A* 109:1159–1164. <https://doi.org/10.1073/pnas.1109326109>.
 54. Zelezniak A, Andrejev S, Ponomarova O, Mende DR, Bork P, Patil KR. 2015. Metabolic dependencies drive species co-occurrence in diverse microbial communities. *Proc Natl Acad Sci U S A* 112:6449–6454. <https://doi.org/10.1073/pnas.1421834112>.
 55. Kitano H. 2004. Biological robustness. *Nat Rev Genet* 5:826–837. <https://doi.org/10.1038/nrg1471>.
 56. Ho A, Mendes LW, Lee HJ, Kaupper T, Mo Y, Poehlein A, Bodelier PLE, Jia Z, Horn MA. 2020. Response of a methane-driven interaction network to stressor intensification. *FEMS Microbiol Ecol* 96:faa180. <https://doi.org/10.1093/femsec/faa180>.
 57. Krause SMB, Meima-Franke M, Veraart AJ, Ren G, Ho A, Bodelier PLE. 2018. Environmental legacy contributes to the resilience of methane consumption in a laboratory microcosm system. *Sci Rep* 8:8862. <https://doi.org/10.1038/s41598-018-27168-9>.
 58. Iguchi H, Yurimoto H, Sakai Y. 2011. Stimulation of methanotrophic growth in cocultures by cobalamin excreted by rhizobia. *Appl Environ Microbiol* 77:8509–8515. <https://doi.org/10.1128/AEM.05834-11>.
 59. Murase J, Frenzel P. 2007. A methane-driven microbial food web in a wetland rice soil. *Environ Microbiol* 9:3025–3034. <https://doi.org/10.1111/j.1462-2920.2007.01414.x>.
 60. Muñoz-Dorado J, Marcos-Torres FJ, García-Bravo E, Moraleda-Muñoz A, Pérez J. 2016. Myxobacteria: moving, killing, feeding, and surviving together. *Front Microbiol* 7:781. <https://doi.org/10.3389/fmicb.2016.00781>.
 61. Qiu Q, Noll M, Abraham W-R, Lu Y, Conrad R. 2008. Applying stable isotope probing of phospholipid fatty acids and rRNA in a Chinese rice field

- to study activity and composition of the methanotrophic bacterial communities *in situ*. ISME J 2:602–614. <https://doi.org/10.1038/ismej.2008.34>.
62. Morris BEL, Henneberger R, Huber H, Moissi-Eichinger C. 2013. Microbial syntrophy: interaction for the common good. FEMS Microbiol Rev 37:384–406. <https://doi.org/10.1111/1574-6976.12019>.
 63. Johnson WM, Alexander H, Bier RL, Miller DR, Muscarella ME, Pitz KJ, Smith H. 2020. Auxotrophic interactions: a stabilizing attribute of aquatic microbial communities? FEMS Microbiol Ecol 96:fiab115. <https://doi.org/10.1093/femsec/fiaa115>.
 64. Kwon G, Kim H, Song C, Jahng D. 2019. Co-culture of microalgae and enriched nitrifying bacteria for energy-efficient nitrification. Biochemical Engineering J 152:107385. <https://doi.org/10.1016/j.bej.2019.107385>.
 65. Wubs ERJ, van der Putten WH, Bosch M, Bezemer TM. 2016. Soil inoculation steers restoration of terrestrial ecosystems. Nat Plants 2:16107. <https://doi.org/10.1038/nplants.2016.107>.
 66. Neufeld JD, Vohra J, Dumont MG, Lueders T, Manefield M, Friedrich MW, Murrell JC. 2007. DNA stable-isotope probing. Nat Protoc 2:860–866. <https://doi.org/10.1038/nprot.2007.109>.
 67. Gadkari D. 1984. Influence of the herbicides goltix and sencor on nitrification. Zentralblatt für Mikrobiologie 139:623–631. [https://doi.org/10.1016/S0232-4393\(84\)80056-6](https://doi.org/10.1016/S0232-4393(84)80056-6).
 68. Horn MA, Ihssen J, Matthies C, Schramm A, Acker G, Drake HL. 2005. *Dechloromonas denitrificans* sp. nov., *Flavobacterium denitrificans* sp. nov., *Paenibacillus anaericanus* sp. nov. and *Paenibacillus terrae* strain MH72, N₂O-producing bacteria isolated from the gut of the earthworm *Aporrectodea caliginosa*. Int J Syst Evol Microbiol 55:1255–1265. <https://doi.org/10.1099/ijs.0.63484-0>.
 69. Kolb S, Knief C, Stubner S, Conrad R. 2003. Quantitative detection of methanotrophs in soil by novel *pmoA*-targeted real-time PCR assays. Appl Environ Microbiol 69:2423–2429. <https://doi.org/10.1128/aem.69.5.2423-2429.2003>.
 70. Ho A, Lee HJ, Reumer M, Meima-Franke M, Raaijmakers C, Zweers H, de Boer W, van der Putten WH, Bodelier PLE. 2019. Unexpected role of canonical aerobic methanotrophs in upland agricultural soils. Soil Biol Biochem 131:1–8. <https://doi.org/10.1016/j.soilbio.2018.12.020>.
 71. Ho A, Lüke C, Cao Z, Frenzel P. 2011. Ageing well: methane oxidation and methane oxidizing bacteria along a chronosequence of 2000 years. Environ Microbiol Rep 3:738–743. <https://doi.org/10.1111/j.1758-2229.2011.00292.x>.
 72. Ho A, Ijaz UZ, Janssens TKS, Ruijs R, Kim SY, de Boer W, Termorshuizen A, van der Putten WH, Bodelier PLE. 2017. Effects of bio-based residue amendments on greenhouse gas emission from agricultural soil are stronger than effects of soil type with different microbial community composition. GCB Bioenergy 9:1707–1720. <https://doi.org/10.1111/gcbb.12457>.
 73. Zhang J, Kobert K, Flouri T, Stamatakis A. 2014. PEAR: a fast and accurate Illumina Paired-End reAd mergeR. Bioinformatics 30:614–620. <https://doi.org/10.1093/bioinformatics/btt593>.
 74. Callahan B. 2017. Rdp taxonomic training data formatted for Dada2 (Rdp trainset 16/Release 11.5).
 75. Quast C, Pruesse E, Yilmaz P, Gerken J, Schweer T, Yarza P, Peplies J, Glöckner FO. 2013. The SILVA ribosomal RNA gene database project: improved data processing and web-based tools. Nucleic Acids Res 41: D590–D596. <https://doi.org/10.1093/nar/gks1219>.
 76. Hammer Ø, Harper DAT, Ryan PD. 2001. PAST: Paleontological statistics software package for education and data analysis. Palaeontologia Electronica 4(1):4.
 77. Parks DH, Tyson GW, Hugenholtz P, Beiko RG. 2014. STAMP: statistical analysis of taxonomic and functional profiles. Bioinformatics 30:3123–3124. <https://doi.org/10.1093/bioinformatics/btu494>.
 78. Bastian M, Heymann S, Jacomy M. 2009. Gephi: an open source software for exploring and manipulating networks, p. 361–362. In Third International AAAI Conference on Weblogs and Social Media.
 79. Newman MEJ. 2003. The structure and function of complex networks. SIAM Rev 45:167–256. <https://doi.org/10.1137/S003614450342480>.
 80. Kaupper T, Mendes LW, Lee HJ, Mo Y, Poehlein A, Jia Z, Horn MA, Ho A. 2021. When the going gets tough: emergence of a complex methane-driven interaction network during recovery from desiccation-rewetting. Soil Biol Biochem 153:108109. <https://doi.org/10.1016/j.soilbio.2020.108109>.